Death in the taste bud: engulfment of dying taste receptor cells by glial-like Type I cells

Abbreviated Title: **Glial-like Type I cells engulf dying murine taste cells**

Courtney E. Wilson, Robert S. Lasher, Ernesto Salcedo, Ruibiao Yang, Yannick Dzowo, John C. Kinnamon, Thomas E. Finger

Rocky Mountain Taste & Smell Center, Department of Cell and Developmental Biology, University of Colorado School of Medicine, CU Anschutz Medical Campus, Aurora, CO 80045

Corresponding author: courtney.wilson@cuanschutz.edu

This work was supported by National Institutes of Health National Institute on Deafness and Other Communication Disorders grants R01 DC017679, R01 DC014728, and R21 DC013186. The authors would like to acknowledge Dr. Graham Kidd and Emily Benson at the Lerner Research Institute at the Cleveland Clinic for their contribution to the data acquisition, which lead to this manuscript.

Number of pages: 42

Number of figures: 10

Number of tables: 1

Number of words:

Abstract: 249

Introduction: 800

Discussion: 1699

Abstract

Taste buds comprise 50-100 epithelial derived cells, including glial-like cells (Type I) and two types of receptor cells (Types II and III). All of these taste cells are renewed throughout the life of an organism from a pool of uncommitted basal cells. Immature cells enter the bud at its base, maturing into one of the three mature cell types. How taste cells die and/or exit the bud, as well as the role of the glial-like cells in this process, remains unclear. Here we present morphological data obtained through Serial Blockface Scanning Electron Microscopy of murine circumvallate taste buds, revealing taste cells at the end of their life. Cells we identify as dying share morphological features typical of apoptosis: swollen endoplasmic reticulum, large lysosomes, degrading organelles, distended outer nuclear membranes, heterochromatin reorganization, cell shrinkage, and cell and/or nuclear fragmentation. Most early stage dying cells have Type II cell morphologies, while a few display Type III cell features. Many dying cells maintain contacts with nerve fibers, but those postsynaptic fibers often appear to be detached from the main trunk of an afferent nerve. Dying cells, like mature Type II and III taste cells, are surrounded by glial-like Type I cells. In many instances Type I cells appear to be engulfing their dying neighbors, suggesting for them a novel, phagocytic role. Surprisingly, virtually no Type I cells display features of apoptosis, although they reportedly have the shortest residence time in taste buds. The ultimate fate of Type I cells therefore remains unknown.

Keywords: cell death, taste buds, electron microscopy, glial-like, engulfment, synapse, apoptosis

Table of Contents Entry

Main Points:

1. Dying taste cells display morphologies consistent with apoptosis.
2. Glial-like Type I cells engulf dying neighbors, perhaps acting as “undertakers.”
3. We find no dying Type I cells—all early dying cells are taste transducing Type II or III cells.

52 **Introduction**

53 The peripheral sensory organs for hearing, balance, and taste all contain glial-like cell
54 populations as well as secondary sensory cells involved directly in transduction. These
55 glial-like cells share many features with astrocytes in the CNS including: uptake and
56 inactivation of neurotransmitters (e.g. expression of GLAST, ectoNTPDase) (Furness and
57 Lehre 1997; Glowatzki et al., 2006; Vlajkovic et al., 2002), regulation of ionic
58 environment (K^+ uptake and extrusion) (Li et al., 2012), and metabolic and structural
59 support. Many of these molecular characteristics are also shared by the Muller glial cells
60 of the retina (Bringmann et al., 2009; Wang et al., 2017). In taste buds, the glial-like cells
61 are identified as Type I cells in contradistinction to the Type II and Type III cells involved
62 in transduction of potential taste substances. Type I cells express GLAST (Lawton et al.,
63 2000) and ectoATPase (Bartel et al., 2006), and are implicated in the regulation of
64 potassium ion flux and extracellular neurotransmitter levels (Dvoryanchikov et al., 2009;
65 Rodriguez et al., 2021). Unlike the glial-like cells of other sensory organs, Type I taste
66 cells are thought to have a short life span, being repeatedly replaced over the span of
67 several weeks like the other cells in the bud (Farbman, 1980; Perea-Martinez et al.,
68 2013).

69

70 To maintain a stable population, taste buds must lose and gain cells at roughly the same
71 rate. Organisms rid themselves of aging or unhealthy cells by three general mechanisms:
72 apoptosis, autophagy, and necrosis (D'Arcy, 2019). Apoptosis is a form of programmed
73 cell death resulting in characteristic ultrastructural changes: chromatin condensation,

74 nuclear fragmentation, cell shrinkage, and ultimately the formation of apoptotic bodies
75 that fragment off the cell. In contrast, in autophagy, which can either protect or kill a
76 cell, macroproteins and organelles are sequestered into autophagosomes and are
77 degraded. The process of necrosis may result from acute injury to the cell; necrotic cells
78 swell and rupture, spilling their contents and triggering an inflammatory response
79 (D'Arcy, 2019; Chen et al., 2020). Only a few studies of cell death in the taste bud exist,
80 and all report instances of taste cell apoptosis (Suzuki et al., 1996A; Takeda et al., 1996;
81 Zeng and Oakley, 1999; Zeng et al., 2000; Huang and Lu, 2001; Ueda et al., 2008).
82
83 We examined serial electron micrographs through taste buds obtained by serial
84 blockface scanning electron microscopy (sbfSEM) to identify ultrastructural signs of cell
85 death, expecting to find dying glial-like Type I cells as well as taste-transducing Type II
86 and III cells in proportion to their respective populations and rates of replacement
87 within taste buds. The three mature taste cell types are each unique in morphology,
88 lifespan, and function. Glial-like Type I cells constitute ~50% of the mature cells in the
89 bud (Murray et al., 1969; Pumplin et al., 1997; Yang et al., 2020) and have an estimated
90 lifespan of ~7 and ~16 days in rat and mouse, respectively (Farbman, 1980; Perea-
91 Martinez et al., 2013). Type II cells, about one quarter of the cells in a bud, are spindle-
92 shaped receptor cells and live for ~14-30 days (Perea-Martinez et al., 2013; Gross et al.,
93 2017; Yang et al., 2020). Each Type II cell expresses receptors for only one of the
94 classical taste qualities: bitter, sweet, or umami, and perhaps amiloride-dependent
95 sodium taste (Ohmoto et al., 2020). Type II cells communicate to nerve fibers via

96 channel synapses, involving large-pore, voltage-gated channels associated with
97 "atypical" mitochondria (Royer and Kinnamon, 1988; Chaudhari and Roper, 2010;
98 Taruno et al., 2013; Romanov et al., 2018). The other receptor cell type of taste buds,
99 Type III cells, are spindle-shaped cells, which constitute about 15-17% of the mature
100 cells in a bud and are the most long-lived taste cells, with a half-life of at least 22 days
101 (Perea-Martinez et al., 2013). Type III cells transduce ionic taste qualities, i.e. sour and
102 highly salty stimuli, and communicate to nerves via conventional vesicular synapses
103 (Kinnamon et al., 1985; Yee et al., 2001; Huang et al., 2008; Yang et al., 2020). We
104 hypothesize that Type I cells, being the most abundant and shortest-lived cell type in
105 taste buds, would exhibit the clearest signs of apoptosis. Surprisingly, we did not find
106 any glial-like Type I cells with morphological signs of cell death in our datasets. Rather,
107 dying Type II and III taste cells are all at least partially surrounded by Type I taste cells,
108 some quite substantially so. This arrangement and the presence of abundant, large
109 lysosomes in Type I cells adjacent to dying cells suggest that Type I cells, like astrocytes
110 in the CNS (Morizawa et al., 2017; Kono et al., 2021; Zhou et al., 2022), can engulf and
111 degrade dying cells. That we find no evidence of dying Type I cells leaves open the
112 question as to when and how these cells exit the taste bud to be replaced during the
113 lifespan.
114
115 **Methods**
116 *Serial Block Face Scanning Electron Microscopy*

117 As reported previously, Serial Blockface Scanning Electron Microscopy (sbfSEM) [see
118 (Yang et al., 2020)] was used to generate two datasets from adult (>45 days) mouse
119 circumvallate taste buds: DS2, composed of 563 sections, and TF21, composed of 633
120 sections. The data used in the present study were obtained primarily from two complete
121 and one nearly complete taste buds from TF21 (Fig.1). A small number of cells from DS2
122 were also identified as early stage dying cells and more from this dataset were used for
123 analysis of lysosomes. The original image data are freely available at the Electron
124 Microscopy Public Image Archive, part of the European Bioinformatics Institute (EMBL-
125 EBI), in dataset EMPIAR-10331. Every taste cell in each section was assigned a unique
126 identifier and was analyzed using Reconstruct software (Synapse Web Reconstruct,
127 RRID:SCR_002716) (Fiala, 2005) to determine cell type and generate 3D reconstructions.
128
129 *Identifying taste cells*
130 Mammalian taste buds contain three basic types of mature taste cells: Type I, II, and III
131 cells. We identified cells as being part of one of these categories based on several
132 morphological features described in previous studies (Yang et al., 2020) (**Figure 1**). Type
133 I cells tend to have elongate, invaginated nuclei, as well as thin, lamellar processes that
134 extend around and between neighboring taste cells. While they often wrap around and
135 border innervating nerve fibers, they do not display synaptic morphology (either
136 atypical mitochondria or synaptic vesicles) at these sites of contact. The apical structure
137 of Type I cells falls into two main categories: bushy, with many short microvilli, or
138 arboriform, with one main microvillus with smaller microvillar “branches” (Yang et al.,

139 2020). Type II cells are elongate, have a somewhat flattened fusiform shape, and
140 relatively smooth, ovoid nuclei. The majority of Type II cells contain so called "atypical"
141 mitochondria. These large mitochondria are characterized by tubular rather than
142 stacked cristae and exist at points of synaptic contact from Type II cells onto afferent
143 nerve fibers (Royer and Kinnamon 1988; Romanov et al., 2018) (**Figure 1B**). At their
144 apical regions, Type II cells (e.g., **Figure 2A**) generally feature a single, large microvillus
145 that extends far into the taste pore. Type III cells are elongate and spindle-shaped, with
146 a single, large microvillus that extends far into the taste pore and nuclei that are
147 elongate and slightly invaginated (Yee et al., 2001; Yang et al., 2020). They are the only
148 cells in the taste bud that form conventional, vesicular synapses onto afferent nerve
149 fibers. These points of synaptic contact feature clear, 40-60nm diameter vesicles
150 clustered at the plasma membrane region bordering the nerve fiber (**Figure 1C**).
151
152 *Identifying lysosomes*
153 The morphology of lysosomes can vary greatly over time and location in a cell (e.g., Dr.
154 Jastrow's electron microscopic atlas, http://www.drjastrow.de/WAI/EM/EMAtlas.html.)
155 Taste cell lysosomes appear to fall into two categories. The first category contains
156 roughly spherical membrane-bound vesicles of about 150-600 nm in diameter
157 containing packed, electron dense granules. The second category contains larger,
158 irregularly shaped structures up to 1-2 µm in the longest dimension. These larger
159 lysosomes have inclusions of electron dense material embedded in a matrix comprising
160 a combination of somewhat electron dense material and electron lucent material. We

161 segmented profiles of lysosomes in every section of selected cells, being careful not to
162 include any tangential or cross-sections of mitochondria which may have a similar
163 appearance in single sections. Counts of lysosomes were performed using images taken
164 from 3D reconstructions of cells primarily from dataset TF21.
165
166 *Estimating ER distention*
167 To estimate the size of dying cell endoplasmic reticulum regions as compared to those
168 of healthy cells, we chose three healthy and three dying cells at random. In these cells,
169 we randomly chose among sections containing the cell nucleus, using an online random
170 number generator to select the section number, and used Photoshop (Adobe) to
171 measure 5 separate sections of ER at their widest points from each cell. These values
172 were then averaged for our estimates.
173
174 *Nuclear Reconstructions and Display*
175 Nuclear and taste bud perimeter traces were exported from the Reconstruct series files
176 into MATLAB (Mathworks, Natick, MA) using custom MATLAB scripts
177 (https://github.com/salcedoe/Dying_Taste_Cell_analysis). These traces were exported as
178 a series of X, Y, and Z geometric vertices, which were organized in a table and sorted by
179 cell identity and cell type. Vertices from individual nuclei were bound into 3D polyhedral
180 meshes using the alphaShape function and visualized by plotting as 3D surface polygons.
181
182 *Lysosome and Cell Volume Analysis*

183 Cell and lysosomal traces were imported as geometric vertices into MATLAB as
184 described for the nuclear reconstructions. The vertices were then grouped by cell
185 identity and cell type. To determine lysosome size, vertices from lysosome traces were
186 converted into Point Cloud objects using the pointCloud tool from the MATLAB
187 Computer Vision Toolbox. These point clouds were then segmented into distinct
188 lysosome clusters based on a set Euclidean distance using the MATLAB pcsegdist
189 function. Individual lysosome volumes were calculated by converting the lysosome point
190 cloud clusters into 3D polyhedral meshes using the MATLAB alphaShape function, which
191 then calculated the encased volume of each mesh. All generated 3D polyhedral surface
192 meshes were visually inspected for morphological accuracy. Surface defects (e.g. large
193 holes in the surface) were repaired using Manifold plus
194 (https://github.com/hjwdzh/ManifoldPlus) and Meshfix 2.1
195 (https://github.com/MarcoAttene/MeshFix-V2.1). Taste cell volumes were then
196 calculated from these inspected surface meshes. All cell meshes can be found on the
197 github repository in the Lysosome Analysis/cellMeshes folder.
198
199 *Statistical Analysis*
200 MATLAB was used to calculate the statistics for the lysosome sizes. Comparisons
201 between separate cell categories (i.e. healthy Type II cells, early stage dying Type II cells,
202 healthy Type III cells, late stage dying cells, etc.) with regards to lysosome volumes were
203 performed with Kruskal-Wallis and ANOVA tests, depending on whether datasets
204 qualified as skewed by a Kolmogorov-Smirnov test. Comparisons between separate cell

205 categories with regards to cell volumes were performed using estimation statistics on
206 the median difference. (estimationstats.com ; Ho et al., 2019). The results of these cell
207 volume estimation statistics are presented in **Supplemental Figure 1.**
208
209 *Code/Software Accessibility*
210 Code was generated for lysosome volumetric analysis and is readily available on GitHub
211 (https://github.com/salcedoe/Dying_Taste_Cell_analysis).
212
213 **Results**
214 *General features of dying taste cells and their nuclei*
215 The taste cells that we identify as dying share several distinct morphological features
216 that distinguish them from mature taste cells (**Figure 2**). In the cytoplasm of dying cells,
217 abundant, swollen endoplasmic reticulum and large lysosomes are among the most
218 readily apparent and common of these features. The endoplasmic reticulum of dying
219 cells appears swollen in comparison to that of mature taste cells; the width (roughly
220 perpendicular to the longitudinal axis) of ER segments in dying cells is ~250nm, while in
221 healthy cells, the ER width is ~90nm (**Figure 2B, B', C, C'**). Healthy cells contain relatively
222 small lysosomes, with median individual lysosome volumes ranging from 0.005-0.06 μm^3
223 per cell. In contrast, lysosomes in dying cells tend to be larger, with median lysosome
224 volumes ranging from 0.004-0.12 μm^3 per cell (**Figure 2E, F, Figure 4**). Lysosome
225 volumes differed significantly between the six different groups—I, II, III, IV, early dying,
226 and late dying [Kruskal-Wallis test, $H(5, n=3904) = 328.2$, $p<0.0001$]. When we directly

227 compared the lysosomes from healthy and early dying Type II cells in a post-hoc,
228 multiple comparison analysis, we found the lysosomes in the dying cells to be
229 significantly larger than the lysosomes in the healthy cells ($p<0.0001$). Mitochondria in
230 dying cells often display signs of degradation—instead of the stacked cristae of healthy
231 mitochondria or the tubular cristae of atypical mitochondria, mitochondria in dying cells
232 often contain irregular, sparse cristae (**Figure 2G**). Golgi bodies in dying cells, like the
233 endoplasmic reticulum, appear swollen (**Figure 2I, I'**) when compared to those of
234 healthy, mature taste cells (**Figure 2H, H'**). A subset of dying taste cells feature more
235 obvious signs of apoptosis: cell shrinkage and even cell fragmentation into apoptotic
236 bodies (**Figure 2A, D**). We deem these cells "late stage" dying cells, as opposed to the
237 "early stage" dying cells, which are not fragmented and are still identifiable by cell type.
238 Late stage dying cells are smaller than healthy cells, ranging in volume from 403-457
239 μm^3, while healthy Type II and III cells for which volume was measured range from 524-
240 1172 μm^3. Interestingly, early stage dying Type II and III cells tend to be slightly larger
241 than their healthy counterparts as well as late stage dying cells, ranging from 319-1984
242 μm^3 (**Figure 3, Supplementary Figure 1**). Late stage dying cells are fragmented into
243 multiple separate objects. We presume these objects to be fragmented apoptotic
244 bodies when they are in proximity to the main cell body and mirror its cytosolic qualities
245 (**Figure 2D**).
246
247 Nuclei in dying cells likewise differ from those of mature taste cells (**Figure 5**). In dying
248 cells that feature swollen endoplasmic reticulum and large lysosomes, the nuclear

249 membranes exhibit clear, distended regions of separation between the inner and outer
250 nuclear lamellae (**Figure 5B, C**). The degree of nuclear membrane separation varies
251 among dying cells, with individual distended regions ranging from ~160 to 500 nm
252 between the inner and outer leaflets (**Figure 5B, C, E', G'**). Since this intra-membrane
253 region is contiguous with the inner endoplasmic reticular space (Lindenboim et al.,
254 2020), the distended nuclear membrane of dying cells may be an extension of the
255 swollen endoplasmic reticulum, or vice versa. In a small subset of dying cells, nuclei
256 feature accumulations of dense heterochromatin, a common characteristic of apoptotic
257 cells (D'Arcy, 2019; Snigirevskaya and Komissarchik, 2019) (**Figure 5E', G'**). In one cell
258 that appears to have fragmented into multiple apoptotic bodies, the nucleus is likewise
259 fragmented into multiple bodies, which is consistent with caspase-induced breakdown
260 of nuclear lamins (for review, Fink and Cookson, 2005) (**Figure 5E, E'**). Other nuclei in
261 late stage dying cells possess large invaginations, which are perhaps harbingers to
262 nuclear fragmentation (**Figure 5G, G'**).
263
264 *Synapses in dying cells*
265 The genesis and degeneration of taste cells necessitates remodeling of synaptic contacts
266 and nerve fibers. To ascertain whether dying cells might still be communicating to taste
267 nerves, we investigated possible synapses between dying cells and afferent nerve fibers.
268 Late stage dying cells did not exhibit structures consistent with synapses onto afferent
269 nerve fibers. At points of contact with nerve fibers, late stage dying cells lacked both the

270 atypical mitochondria that characterize Type II cell synapses onto nerve fibers as well as
271 the pre-synaptic clusters of vesicles characteristic of Type III cell synapses (**Figure 6A**).
272
273 In contrast, most early stage dying cells were Type II cells still showing the presence of
274 atypical mitochondria characteristic of synaptic contacts from this cell type. These
275 atypical mitochondria appeared at sites of contact with nerve fibers, but these nerve
276 fibers did not always exit the taste bud, suggesting nerve fiber fragmentation. This
277 observation suggests that early stage dying Type II cells retain gross synaptic structures,
278 but may not always be capable of signaling information to the CNS since the nerve fiber
279 has fragmented (**Figure 6B, C**) and is no longer connected to the CNS. The atypical
280 mitochondria in early stage dying Type II cells feature irregular, "loose" cristae (**Figure**
281 **6B**) when compared to the tubular cristae of atypical mitochondria in mature, healthy
282 Type II cells (**Figure 1B**).
283 A minority of the early stage dying cells are Type III cells. These cells share similar
284 cytoplasmic quality with early stage dying Type II cells, but lack atypical mitochondria.
285 Instead, at points of contact with nerve fibers, we observe clear, membrane enclosed
286 profiles that are larger than typical synaptic vesicles. Synaptic vesicles in healthy Type III
287 cells range from 40-60 nm (Yang et al., 2020); membrane-bound objects at the site of
288 contact between a dying Type III cell and a bordering nerve fiber range from ~30-300
289 nm. We tentatively mark these structures as degrading synaptic contacts, although the
290 occurrence of signal transmission at these sites is unknowable with our current methods
291 (**Figure 6D, E**). As with some fibers innervating early stage dying Type II cells, some

292 nerve fibers contacting the putative early stage dying Type III cells do not exit the bud,
293 suggesting nerve terminal fragmentation (**Figure 6F**). In TF21_ TB2, from which we have
294 a complete connectome (Wilson et al., 2022), 4 of 7 (57%) nerve fibers innervating dying
295 cells are fragments that do not appear to exit the bud, while just 8 of 25 (32%) of nerve
296 fibers innervating healthy cells appear to be fragments.
297
298 *Type I cells engulf dying cells*
299 Apoptotic cells elsewhere in the body are generally phagocytosed by elements of the
300 immune system, often prior to the development of apoptotic bodies (D'Arcy, 2019). In
301 the nasal epithelium, which is largely devoid of immune cells, sustentacular cells
302 phagocytose neighboring epithelial cells (Suzuki et al., 1996B). Type I cells are
303 considered the glial-like cells of the taste bud (for review, Chaudhari and Roper 2010).
304 Type I cells possess diaphanous processes that extend around and between neighboring
305 taste cells and are well positioned to engulf dying cells and any apoptotic bodies they
306 might generate. Indeed, we observe signs of Type I cells engulfing dying cells and their
307 fragmented apoptotic bodies (**Figure 7A-C**). In addition, membrane bound objects
308 matching the cytosolic presentation of a dying cell are often seen in the cytoplasm of
309 immediately adjacent Type I cells (**Figure 7C, E**). In regions of Type I cells that border
310 dying cells, lysosomes tend to be larger, much like the lysosomes in the dying cells
311 themselves (**Figure 4, Figure 7D, D''**). The 3 largest individual lysosomes in Type I cells
312 range from 7.5-9.1 μm^3, which is several times the volume of the median volume
313 lysosomes in either healthy or dying cells. In one case, a Type I cell that neighbors an

314 early stage dying cell appears to have engulfed large, vacuous, membrane enclosed
315 bodies. These bodies closely resemble the cytosolic appearance of the dying cell rather
316 than the Type I cell itself. Thus, we presume this material originated in the dying cell
317 (**Figure 7E**). We have never observed either immune cells or other non-taste cells within
318 the confines of the taste bud that could be involved in the elimination of dying cells.
319
320 *Dying taste cells in the context of the bud*
321 In total, we identify 21 dying cells in 5 different taste buds over two separate datasets.
322 In the two taste buds wholly contained within the segmented block of tissue, 4 out of 84
323 and 5 out of 86 total taste cells appear to be dying according to our previously discussed
324 morphological criteria. Of these dying cells, early stage dying cells are still identifiable as
325 belonging to a mature taste cell type. These cells feature some, but not all,
326 characteristics of dying cells. They tend to display swollen endoplasmic reticulum,
327 degrading mitochondria, blebby nuclear membranes, swollen Golgi bodies, and large
328 lysosomes. Of these early stage cells, most are Type II cells that maintain aspects of Type
329 II cell morphology and atypical mitochondria. The remaining early stage dying cells share
330 qualities with mature Type III cells. No early stage dying cells exhibit Type I cell
331 morphology although Type I cells are the majority of the cells in a taste bud. Late stage
332 dying cells could not be identified as to taste cell subtype, because of the more
333 advanced signs of cell degradation: cell fragmentation, nuclear fragmentation, and
334 notable reorganization of dense regions of heterochromatin in the nucleus. We thus
335 label these cells as “unknown type” (**Figure 8A, Figure 9**).

336

337 *Location of dying cells within the taste bud*

338 Post-mitotic, immature Type IV taste cells are known to enter the taste bud near the
339 basilar membrane and inhabit the bottom 1/3 of the bud (Barlow, 2015; Yang et al.,
340 2020). As they mature, taste cells extend into the upper portions of the bud, eventually
341 reaching the taste pore. We hypothesized that dying cells would be restricted to the
342 upper regions of the taste bud, farther away from their origins in the basal regions of
343 the bud consistent with a general migration from basal to apical within the epithelium.
344 Indeed, the nuclei of dying cells tend to be in the top 1/3 of the taste bud, although
345 taste cells at the upper regions of the bud do not all display hallmarks of degeneration
346 (**Figure 8B**).

347

348 **Discussion**

349 The data we present suggest an apoptotic pathway for the death of Type II and III taste
350 receptor cells (**Figure 9**), but not for glial-like Type I cells. As the receptor cells progress
351 towards death, the ER and Golgi swell, lysosomes enlarge, mitochondrial cristae become
352 disorganized, and the inner and outer leaflets of the nuclear membrane separate
353 (**Figures 2, 4, and 5**). These features are consistent with apoptosis (D'Arcy, 2019;
354 Snigirevskaya and Komissarchik, 2019), and agree with reports of apoptotic markers
355 within taste buds (Zeng and Oakley, 1999; Zeng et al., 2000; Huang and Lu, 2001; Takeda
356 et al., 1996). Early stage dying cells tend to be larger than healthy or late stage cells,
357 indicating that cells swell slightly before late stage cell death (**Figure 3**). As cells progress

358 to the late dying stage, heterochromatin reorganization becomes more pronounced, cell
359 volume reduces, and apoptotic bodies separate from the main cell body (**Figures 2, 3,**
360 **and 5**).
361
362 We conclude that the dying cells we describe are undergoing apoptosis. If taste cells
363 were dying by non-apoptotic methods, we would expect different morphologies. Cells
364 undergoing necrosis would manifest substantial cell swelling, extracellular spillage of
365 cell contents, and infiltration of immune cells (D'Arcy, 2019; Lakshmanan et al., 2022).
366 Instead, we observe cell shrinkage in late stage dying cells, formation of putative
367 apoptotic bodies, and no evidence of immune cell infiltration. Interestingly, early stage
368 dying cells are slightly larger than healthy cells (**Figure 3, Supplementary Figure 1**). That
369 cells swell before shrinking is not necessarily inconsistent with apoptosis. Reduced ATP
370 production on account of degrading mitochondria might disrupt the Na^+/K^+-ATPase,
371 which can result in swelling (Chen et al., 2014). In autophagy, dying cells would form
372 autophagosomes, which sequester and degrade macroproteins and organelles
373 (Eskelinen et al., 2011). We do not observe such structures in dying Type II or III cells,
374 although autophagosome-like structures occasionally appear in Type I cells. However,
375 we cannot determine if these structures indicate cell death or repair.
376
377 In the two complete buds contained within the samples, few cells per bud appear to be
378 undergoing apoptosis: 4 of 84 (4.7%) and 5 of 86 (5.8%). Some previous studies estimate
379 the dying cell population at 1-3 dying cells per bud (Ueda et al., 2008; Huang and Lu,

380 2001; Takeda et al., 1996), while others estimate it at ~9 cells per bud (Zeng and Oakley,
381 1999; Zeng et al., 2000) (**Table 1**). Our observed prevalence of apoptotic cells may be
382 higher than the lower estimates due to the relatively short period (1-3 hrs) during which
383 an apoptotic cell is positive for classical apoptotic markers, i.e. TUNEL and ssDNA
384 (Gavrieli et al., 1992). The studies that estimated a larger dying cohort used p53 and
385 Caspase-2 as markers, both of which are initiating apoptotic factors whose presence
386 likely precedes the morphological changes we report (Zeng and Oakley 1999; Zeng et al.,
387 2000, Bouchier-Hayes and Green, 2012). Beidler and Smallman (1965) reported that rat
388 taste buds lose approximately half their cells every 10 days. If mouse taste buds are
389 similar, we expect 4-5 dying cells per day in a bud of 80-100 cells. Our results are
390 consistent with this estimate.
391
392 Of early stage dying taste cells, the majority are Type II cells and a few are Type III
393 cells—we observe no dying Type I cells. Buds contain fewer Type III than Type II cells,
394 and Type III cells are the longest-lived, making it less likely that we would observe them
395 dying in a single snapshot of a dynamic organ. Surprisingly, we do not observe apoptotic
396 Type I cells. Type I cells are the most common cell type (~50% of all cells; Yang et al.,
397 2020), and are described as the shortest-lived (Farbman, 1980; Perea-Martinez et al.,
398 2013; Gross et al., 2017; Yang et al., 2020). If a bud contains ~100 cells, we expect ~50 to
399 be Type I cells. If, as according to the estimates of Beidler and Smallman (1965) and
400 Yang et al (2020), half of this population is renewed every 10 days, then we would
401 expect ~2.5 Type I cells dying per day in each taste bud. Since this estimate is based on

402 the entire taste cell population, and Type I cells reportedly have the shortest lifespan
403 (Farbman, 1980; Hamamichi et al., 2006; Perea-Martinez et al., 2013; Gross et al., 2017),
404 the estimate is likely conservative. However, we do not observe apoptotic Type I cells.
405 What then, is their ultimate fate? Ueda and colleagues reported a population of
406 apoptotic cells interpreted as Type I cells in rats (Ueda et al., 2008). The marker used to
407 identify these cells (human blood antigen H) is, however, not specific to Type I cells
408 (Ueda et al., 2003). Other estimates of Type I cell lifespans are based on perdurance of
409 nucleotide labeling during progenitor cell division; Farbman (1980) estimated "dark"
410 cells (an earlier term apparently equivalent to Type I cells) to have a lifespan of ~7 days,
411 and Perea-Martinez (2013) and colleagues found cells lacking Type II or III markers
412 (presumed Type I cells) to have a ~16 day lifespan. If Type I cells are exiting the bud
413 rather than dying, previous studies would not necessarily capture that process.
414 Conceivably, Type I cells may exit the taste bud apically or laterally, to be eventually
415 sloughed off the lingual epithelium with non-taste epithelial cells. Alternatively, Type I
416 cells may be dying too quickly to capture in our sampling paradigm, or may die via an
417 alternative cell death process which shows no obvious morphological features. We do
418 occasionally observe autophagosome-like profiles in Type I cells, but cannot determine
419 whether these structures indicate cell death, cell repair, or phagocytosis of neighboring
420 dying cells. Possibly, the Type I cells undergo autophagy following phagocytosis of other
421 dying cells. The cells we describe as late stage dying cells could include Type I cells, but
422 are more rare than expected. A final alternative is that Type I cells are more long-lived
423 than previously estimated, and that Type II and III cells turn over while the Type I cell

population remains relatively constant. Our data do not resolve how and whether Type I cells die or otherwise exit the taste bud.

Early stage dying Type II and III cells feature synaptic structures in various stages of degradation, suggesting impaired signaling to nerves. Moreover, these dying cells often contact postsynaptic nerve fibers that, seemingly, do not exit the bud and thus cannot signal to the CNS. In the face of wholesale turnover of taste receptor cells, taste nerves are constantly remodeling (Whiddon et al., 2023). Large “end-bulbs” are associated with nerve branch retraction (Zaidi et al., 2016; Whiddon et al., 2023) and we occasionally observe enlarged nerve processes near late stage dying cells (**Figure 6A**). More often, synapses from dying cells contact nerve fiber fragments (**Figure 6B-F**). Considering these data, we hypothesize that nerve fiber fragments that receive synapses from early stage dying cells become separated from their trunk nerve fibers as a part of the remodeling process. Such nerve fragments are not reported by Whiddon et al (2023), who rely on sparse GFP label to follow individual fibers within a taste bud. A possible explanation for this discrepancy is that once a nerve fiber fragment detaches from the nerve trunk, it’s ability to maintain pH homeostasis degrades, which would cause cytoplasmic acidification and would likely quench the GFP fluorescence (Roberts et al., 2016). We cannot, however, rule out the possibility that these nerve fiber fragments are attached to fibers exiting the bud, but that our data do not allow us to accurately trace the full nerve profile. In our dataset, it can be challenging to follow processes with diameters

445 less than 70 nm (the section thickness) as they wend their way between other cell and
446 fiber processes.
447
448 Type I cells play a crucial physiological role in taste buds, analogous to the role of
449 astrocytes in regulating neural transmission at tripartite synapses in the brain (Araque et
450 al., 1999; Dando et al., 2012; Kataoka et al., 2012; Rodriguez et al., 2021). Our data
451 present a novel role for glial-like Type I cells in the homeostasis of taste bud structure,
452 i.e. Type I cells engulf and remove neighboring apoptotic cells. In many tissues, immune
453 cells fill this phagocytic role (D'Arcy, 2019) but we find no evidence for immune cells
454 within taste buds. Type I cells, considered the glial-like support cells of the taste bud, are
455 well poised for a phagocytic role. Type I cells most directly resemble astrocytes of the
456 CNS—they degrade excess ATP, a taste neurotransmitter, and appear to sense and
457 facilitate signaling at taste synapses (Roper, 2013; Rodriguez et al., 2021). While not the
458 primary phagocytic glia in the CNS, astrocytes phagocytose and degrade synapses, distal
459 dendrites of injured neurons, and dying microglia (Morizawa et al., 2017; Kono et al.,
460 2021; Zhou et al., 2022). In the olfactory system, glial-like Olfactory Ensheathing Cells
461 regularly phagocytose and degrade dying olfactory neurons which, like taste buds, make
462 up a sensory cell population that is renewed repeatedly (Nazareth et al., 2021).
463 Precedence also exists for supporting cells in sensory epithelia engulfing dying cells, as
464 in the olfactory epithelium (Suzuki et al., 1996B). Previous studies found Type I taste
465 cells containing large, dense bodies within their cytosol (Takeda et al., 1996; Farbman,
466 1969; Fujimoto and Murray 1970; Olivieri-Sangiacomo, 1970; Farbman, 1985). Our data

467 are consistent with these observations, leading us to the hypothesis that Type I cells
468 phagocytose and degrade debris from apoptotic Type II and III cells.
469
470 Our data point to apoptosis as the major mechanism of death for murine taste cells. The
471 dying cells we identify feature several hallmarks of apoptosis, and can be categorized
472 into either early or late stages of death. Those that retain synaptic contacts with nerve
473 fibers during early stages of cell death are likely impaired in their ability to communicate
474 to the CNS, as many of their target nerve fibers are fragmented. Type I cells appear to
475 engulf dying cells, identifying a novel, phagocytic role for Type I taste cells. We do not,
476 however, identify morphologically recognizable Type I cells in the process of cell death.
477 Whether, how, and when Type I cells die or exit the taste bud remains unclear.
478

479 **References**

480 Araque, A., Parpura, V., Sanzgiri, R. P., & Haydon, P. G. (1999). Tripartite synapses: glia, the
481 unacknowledged partner. *Trends Neurosci*, *22*(5), 208-215.
482

483 Barlow LA (2015). Progress and renewal in gustation: new insights into taste bud development.
484 *Development*, *142*(21), 3620-3629.
485

486 Bartel DL, Sullivan SL, Lavoie EG, Sevigny J, Finger TE. 2006. Nucleoside triphosphate
487 diphosphohydrolase-2 is the ecto-ATPase of type I cells in taste buds. The Journal of
488 comparative neurology 497: 1-12.

489

490 Beidler LM, Smallman RL (1965). Renewal of cells within taste buds. J Cell Biol, 27(2),
491 263-272.
492

493 Bouchier-Hayes, L., & Green, D. R. (2012). Caspase-2: The orphan caspase. *Cell Death Differ*,
494 *19*(1), 51-57.
495

496 Bringmann A, Pannicke T, Biedermann B, Francke M, Iandiev I, Grosche J, Wiedemann P,
497 Albrecht J, Reichenbach A. 2009. Role of retinal glial cells in neurotransmitter uptake and
498 metabolism. Neurochem Int 54: 143-160.

499

500 Chaudhari N, & Roper SD (2010). The cell biology of taste. J Cell Biol, 190(3), 285-296.

501

502 Chen D, Song M, Mohamad O, Yu SP (2014). Inhibition of Na+/K+-ATPase induces hybrid

503 cell death and enhanced sensitivity to chemotherapy in human glioblastoma cells. BMC

504 Cancer, 14, 716.

505

506 Chen Y, Hua Y, Li X, Arslan IM, Zhang, W., & Meng, G. (2020). Distinct Types of Cell Death

507 and the Implication in Diabetic Cardiomyopathy. Front Pharmacol, 11, 42.

508

509 Clapp TR, Medler KF, Damak S, Margolskee RF, Kinnamon SC (2006). Mouse taste cells

510 with G protein-coupled taste receptors lack voltage-gated calcium channels and SNAP-

511 25. BMC Biol, 4, 7.

512

513 Dando, R., Dvoryanchikov, G., Pereira, E., Chaudhari, N., & Roper, S. D. (2012). Adenosine

514 enhances sweet taste through A2B receptors in the taste bud. *J Neurosci*, *32*(1), 322-330.

515

516 D'Arcy MS (2019). Cell death: a review of the major forms of apoptosis, necrosis and

517 autophagy. Cell Biol Int, 43(6), 582-592.

518

519 Dvoryanchikov G, Sinclair MS, Perea-Martinez I, Wang T, Chaudhari N. 2009. Inward

520 rectifier channel, ROMK, is localized to the apical tips of glial-like cells in mouse taste

521 buds. The Journal of comparative neurology 517: 1-14.

522

523 Eskelinen EL, Reggiori F, Baba M, Kovacs AL, Seglen PO (2011). Seeing is believing: the
524 impact of electron microscopy on autophagy research. Autophagy, 7(9), 935-956.

525

526 Farbman AI (1969). Fine structure of degenerating taste buds after denervation. Journal
527 of Embryology and Experimental Morphology, 22(1), 55-68.

528

529 Farbman AI (1980). Renewal of taste bud cells in rat circumvallate papillae. Cell Tissue
530 Kinet, 13(4), 349-357.

531

532 Farbman AI, Hellekant G, Nelson A (1985). Structure of taste buds in foliate papillae of
533 the rhesus monkey, Macaca mulatta. Am J Anat, 172(1), 41-56.

534

535 Fiala JC (2005). Reconstruct: a free editor for serial section microscopy. J Microsc, 218(Pt
536 1), 52-61.

537

538 Fink SL, Cookson BT (2005). Apoptosis, pyroptosis, and necrosis: mechanistic description
539 of dead and dying eukaryotic cells. Infect Immun, 73(4), 1907-1916.

540

541 Fujimoto S, Murray RG (1970). Fine structure of degeneration and regeneration in
542 denervated rabbit vallate taste buds. Anat Rec, 168(3), 383-413.

543

544 Furness DN, Lehre KP. 1997. Immunocytochemical localization of a high-affinity
545 glutamate-aspartate transporter, GLAST, in the rat and guinea-pig cochlea. Eur J Neurosci
546 9: 1961-1969.

547

548 Gavrieli Y, Sherman Y, Ben-Sasson SA (1992). Identification of programmed cell death in
549 situ via specific labeling of nuclear DNA fragmentation. J Cell Biol, 119(3), 493-501.

550

551 Glowatzki E, Cheng N, Hiel H, Yi E, Tanaka K, Ellis-Davies GC, Rothstein JD, Bergles DE.
552 2006. The glutamate-aspartate transporter GLAST mediates glutamate uptake at inner
553 hair cell afferent synapses in the mammalian cochlea. J Neurosci 26: 7659-7664.

554

555 Gross L, Scott JK, Castillo Azofeifa D, Gaillard D, Barlow LA (2017). Molecular genetic
556 lineage tracing of taste bud cells in adult mice. AChemS, Bonita Springs, FL.

557

558 Hamamichi R, Asano-Miyoshi M, Emori Y (2006). Taste bud contains both short-lived and
559 long-lived cell populations. Neuroscience, 141(4), 2129-2138.

560

561 Ho J, Tumkaya T, Aryal S, Choi H, Claridge-Chang A (2019). Moving beyond P values: data
562 analysis with estimation graphics. Nat Methods, 16(7), 565-566.

563

564 Huang YA, Maruyama Y, Stimac R, Roper SD (2008). Presynaptic (Type III) cells in mouse
565 taste buds sense sour (acid) taste. J Physiol, 586(12), 2903-2912.
566
567 Huang YJ, Lu KS (2001). TUNEL staining and electron microscopy studies of apoptotic
568 changes in the guinea pig vallate taste cells after unilateral glossopharyngeal
569 denervation. Anat Embryol (Berl), 204(6), 493-501.
570
571 Kataoka, S., Baquero, A., Yang, D., Shultz, N., Vandenbeuch, A., Ravid, K., Kinnamon, S. C., &
572 Finger, T. E. (2012). A2BR adenosine receptor modulates sweet taste in circumvallate taste
573 buds. *PLoS One*, *7*(1), e30032.
574
575 Kinnamon JC, Taylor BJ, Delay RJ, Roper SD (1985). Ultrastructure of mouse vallate taste
576 buds. I. Taste cells and their associated synapses. J Comp Neurol, 235(1), 48-60.
577
578 Kono, R., Ikegaya, Y., & Koyama, R. (2021). Phagocytic Glial Cells in Brain Homeostasis. *Cells*,
579 *10*(6).
580
581 Lakshmanan HG, Miller E, White-Canale A, McCluskey LP (2022). Immune responses in
582 the injured olfactory and gustatory systems: a role in olfactory receptor neuron and
583 taste bud regeneration? Chem Senses, 47.
584

585 Lawton DM, Furness DN, Lindemann B, Hackney CM. 2000. Localization of the
586 glutamate-aspartate transporter, GLAST, in rat taste buds. Eur J Neurosci 12: 3163-3171.
587

588 Li X, Surguchev A, Bian S, Navaratnam D, Santos-Sacchi J. 2012. Extracellular chloride
589 regulation of Kv2.1, contributor to the major outward Kv current in mammalian outer
590 hair cells. Am J Physiol Cell Physiol 302: C296-306.
591

592 Lindenboim L, Zohar H, Worman HJ, Stein R (2020). The nuclear envelope: target and
593 mediator of the apoptotic process. Cell Death Discov, 6, 29.
594

595 Medler KF, Margolskee RF, Kinnamon SC (2003). Electrophysiological characterization of
596 voltage-gated currents in defined taste cell types of mice. J Neurosci, 23(7), 2608-2617.
597

598 Morizawa YM, Hirayama Y, Ohno N, Shibata S, Shigetomi E, Sui Y, Nabekura J, Sato K,
599 Okajima F, Takebayashi H, Okano H, Koizumi S. 2017. Reactive astrocytes function as
600 phagocytes after brain ischemia via ABCA1-mediated pathway. Nature communications
601 8: 28.
602

603 Murray RG, Murray A, Fujimoto S (1969). Fine structure of gustatory cells in rabbit taste
604 buds. J Ultrastruct Res, 27(5), 444-461.

605

606 Nazareth, L., St John, J., Murtaza, M., & Ekberg, J. (2021). Phagocytosis by Peripheral Glia:
607 Importance for Nervous System Functions and Implications in Injury and Disease. *Front Cell Dev*
608 *Biol*, *9*, 660259.

609

610 Ohman LC, Krimm RF (2021). Whole-Mount Staining, Visualization, and Analysis of
611 Fungiform, Circumvallate, and Palate Taste Buds. J Vis Exp(168).

612

613 Ohman LC, Krimm RF (2021). Variation in taste ganglion neuron morphology: insights
614 into taste function and plasticity. Curr Opin Physiol, 20, 134-139.

615

616 Ohmoto M, Jyotaki M, Foskett JK, Matsumoto I (2020). Sodium-Taste Cells Require Skn-
617 1a for Generation and Share Molecular Features with Sweet, Umami, and Bitter Taste
618 Cells. eNeuro, 7(6).

619

620 Olivieri-Sangiacomo C (1970). Ultrastructural modifications of denervated taste buds. Z
621 Zellforsch Mikrosk Anat, 108(3), 397-414.

622

623 Perea-Martinez I, Nagai T, Chaudhari N (2013). Functional cell types in taste buds have
624 distinct longevities. PLoS One, 8(1), e53399.

625

626 Pumplin DW, Yu C, Smith DV (1997). Light and dark cells of rat vallate taste buds are
627 morphologically distinct cell types. J Comp Neurol, 378(3), 389-410.
628
629 Roberts TM, Rudolf F, Meyer A, Pellaux R, Whitehead E, Panke S, Held M (2016).
630 Identification and Characterisation of a pH-stable GFP. Sci Rep, 6, 28166.
631
632 Rodriguez YA, Roebber JK, Dvoryanchikov G, Makhoul V, Roper SD, Chaudhari N (2021).
633 "Tripartite Synapses" in Taste Buds: A Role for Type I Glial-like Taste Cells. J Neurosci,
634 41(48), 9860-9871.
635
636 Romanov RA, Lasher RS, High B, Savidge LE, Lawson A, Rogachevskaja OA, Zhao H,
637 Rogachevsky VV, Bystrova MF, Churbanov GD, Adameyko I, Harkany T, Yang R, Kidd GJ,
638 Marambaud P, Kinnamon JC, Kolesnikov SS, Finger TE (2018). Chemical synapses without
639 synaptic vesicles: Purinergic neurotransmission through a CALHM1 channel-
640 mitochondrial signaling complex. Sci Signal, 11(529).
641
642 Roper SD (2013). Taste buds as peripheral chemosensory processors. Semin Cell Dev
643 Biol, 24(1), 71-79.
644
645 Royer SM, Kinnamon JC (1988). Ultrastructure of mouse foliate taste buds: synaptic and
646 nonsynaptic interactions between taste cells and nerve fibers. J Comp Neurol, 270(1),
647 11-24, 58-19.

648

649 Snigirevskaya ES, Komissarchik YY (2019). Ultrastructural traits of apoptosis. Cell Biol Int,
650 43(7), 728-738.
651

652 Suzuki Y, Takeda M, Farbman AI (1996). Supporting cells as phagocytes in the olfactory
653 epithelium after bulbectomy. J Comp Neurol, 376(4), 509-517.
654

655 Suzuki Y, Takeda M, Obara N, Nagai Y (1996). Phagocytic cells in the taste buds of rat
656 circumvallate papillae after denervation. Chem Senses, 21(4), 467-476.
657

658 Takeda M, Suzuki Y, Obara N, Nagai Y (1996). Apoptosis in mouse taste buds after
659 denervation. Cell Tissue Res, 286(1), 55-62.
660

661 Taruno A, Vingtdeux V, Ohmoto M, Ma Z, Dvoryanchikov G, Li A, Adrien L, Zhao H, Leung
662 S, Abernethy M, Koppel J, Davies P, Civan MM, Chaudhari N, Matsumoto I, Hellekant G,
663 Tordoff MG, Marambaud P, Foskett JK (2013). CALHM1 ion channel mediates purinergic
664 neurotransmission of sweet, bitter and umami tastes. Nature, 495(7440), 223-226.
665

666 Ueda K, Fujii M, El-Sharaby A, Honma S, Wakisaka S (2003). Human blood group antigen
667 H is not the specific marker for type I cells in the taste buds. Arch Histol Cytol, 66(5),
668 469-473.
669

670 Ueda K, Ichimori Y, Maruyama H, Murakami Y, Fujii M, Honma S, Wakisaka S (2008).
671 Cell-type specific occurrence of apoptosis in taste buds of the rat circumvallate papilla.
672 Arch Histol Cytol, 71(1), 59-67.
673
674 Vlajkovic SM, Thorne PR, Sévigny J, Robson SC, Housley GD. 2002. NTPDase1 and
675 NTPDase2 immunolocalization in mouse cochlea: implications for regulation of p2
676 receptor signaling. The journal of histochemistry and cytochemistry : official journal of
677 the Histochemistry Society 50: 1435-1442.
678
679 Wang J, O'Sullivan ML, Mukherjee D, Puñal VM, Farsiu S, Kay JN. 2017. Anatomy and
680 spatial organization of Müller glia in mouse retina. Journal of Comparative Neurology
681 525: 1759-1777.
682
683 Whiddon ZD, Marshall JB, Alston DC, McGee AW, Krimm RF (2023). Rapid structural
684 remodeling of peripheral taste neurons is independent of taste cell turnover. PLoS Biol,
685 21(8), e3002271.
686
687 Wilson CE, Lasher RS, Yang R, Dzowo Y, Kinnamon JC, Finger TE (2022). Taste Bud
688 Connectome: Implications for Taste Information Processing. J Neurosci, 42(5), 804-816.
689

690 Yang R, Crowley HH, Rock ME, Kinnamon JC (2000). Taste cells with synapses in rat
691 circumvallate papillae display SNAP-25-like immunoreactivity. J Comp Neurol, 424(2),
692 205-215.
693
694 Yang R, Dzowo YK, Wilson CE, Russell RL, Kidd GJ, Salcedo E, Lasher RS, Kinnamon JC,
695 Finger TE (2020). Three-dimensional reconstructions of mouse circumvallate taste buds
696 using serial blockface scanning electron microscopy: I. Cell types and the apical region of
697 the taste bud. J Comp Neurol, 528(5), 756-771.
698
699 Yee CL, Yang R, Bottger B, Finger TE, Kinnamon JC (2001). "Type III" cells of rat taste
700 buds: immunohistochemical and ultrastructural studies of neuron-specific enolase,
701 protein gene product 9.5, and serotonin. J Comp Neurol, 440(1), 97-108.
702
703 Zaidi FN, Whitehead MC (2006). Discrete innervation of murine taste buds by peripheral
704 taste neurons. J Neurosci, 26(32), 8243-8253.
705
706 Zeng Q, Oakley B (1999). p53 and Bax: putative death factors in taste cell turnover. J
707 Comp Neurol, 413(1), 168-180.
708
709 Zeng, Q., Kwan, A., & Oakley, B. (2000). Gustatory innervation and bax-dependent caspase-2:
710 participants in the life and death pathways of mouse taste receptor cells. *J Comp Neurol*,
711 *424*(4), 640-650.

Zhou, T., Li, Y., Li, X., Zeng, F., Rao, Y., He, Y., Wang, Y., Liu, M., Li, D., Xu, Z., Zhou, X., Du, S., Niu, F., Peng, J., Mei, X., Ji, S. J., Shu, Y., Lu, W., Guo, F.,…Peng, B. (2022). Microglial debris is cleared by astrocytes via C4b-facilitated phagocytosis and degraded via RUBICON-dependent noncanonical autophagy in mice. *Nat Commun*, *13*(1), 6233.

718 Table 1. Reported numbers of dying cells in taste buds.

Citation	Animal model	Death identification method	Observed dying cells per section	If bud = 40 µm across, dying cells/bud
Ueda et al 2008	Rat	ssDNA stain	1.2 cells / 16 µm section	~3
Zeng & Oakley 1999	Mouse	p53 (early death signal)	11.4%	11.4% (~9 cells)
Zeng et al 2000	Mouse	Caspase-2 (protease)	11% +/- 0.8%	11% (~9 cells)
Huang & Lu 2001	Guinea pig	Tunel stain	~1-2 tunel+ cells / 20 µm section	2-4
Takeda et al 1996	Mouse	Tunel stain	~0.14 tunel+ cells / 6 µm section	0.93

719

720

721 **Figure 1. Taste cell types and synapses in murine circumvallate taste buds. A.** Electron
722 micrograph of a circumvallate mouse taste bud with overlaid individual reconstructions
723 of a Type I cell (green), Type II cell (blue), Type III cell (red), and Type IV immature cell
724 (purple). Scale bar is 10 µm. **B.** Micrograph of the channel synapse between a Type II cell
725 (blue) and adjacent nerve fiber (yellow) bordered by a Type I cell (green). Arrows
726 indicate the large, atypical mitochondria characteristic of Type II cell synapses. Scale bar
727 is 1 µm for both **B** and **C**. **C.** Micrograph of the synapse between a Type III cell (red) and
728 adjacent nerve fiber (yellow) bordered by a Type I cell (green). Arrow indicates the
729 cluster of vesicles at the pre-synaptic membrane.
730
731 **Figure 2. Morphological features of healthy and dying taste cells. A.** Reconstruction of
732 a healthy, mature Type II cell (blue) in the taste bud shell (gray). Scale bar is 10 µm. **B.**
733 Micrograph of a healthy Type II cell, with arrows indicating endoplasmic reticulum (ER).
734 Scale bar is 2 µm and applies to **B, C, E,** and **F**. **B'**. Enlarged region of healthy Type II
735 cytosol showing normal ER (arrows). Scale bar is 1 µm. **C.** Micrograph of a dying Type II
736 cell, with arrows indicating examples of swollen endoplasmic reticulum. **C'.** Enlarged
737 region of dying Type II cell cytosol, featuring swollen endoplasmic reticulum. Scale bar is
738 1 µm. **D.** Reconstruction of a dying cell of unknown type (purple) in the taste bud shell
739 (gray). Scale is the same as in **A**. **D'.** Enlarged region of dying taste cell reconstruction in
740 **D**. Arrow indicates the point of separation between the main dying cell and its apical
741 fragment. **E.** Micrograph of healthy Type II cell, with an arrow indicating the only visible
742 lysosome in this cell profile. **F.** Micrograph of a dying Type II cell, with arrows indicating

743 some of the numerous lysosomes apparent in the cell cytosol. **G.** Micrograph depicting
744 two healthy Type I cells (green, left) and a dying Type II cell (purple, right). Arrows
745 indicate mitochondria in healthy cells (left 2) and those of the dying cell (right 4). Scale
746 bar is 1 µm and applies to **G, H, H', I,** and **I'**. **H.** Micrograph of healthy cell cytosol with
747 arrows indicating Golgi bodies. **H'.** Enlarged region of cytosol including a healthy Golgi
748 apparatus. **I.** Micrograph of a dying Type II cell with arrows indicating swollen Golgi
749 bodies. **I'.** Enlarged region of the swollen Golgi apparatus of a dying cell.
750
751 **Figure 3. Cell volumes of taste cells.** Graph depicts total cell volumes of healthy Type II
752 and III cells (left), early dying Type II and III cells (middle, light gray), and late stage dying
753 cells (right, dark gray).
754
755 **Figure 4. Lysosomes in taste cells. A.** Reconstructions of selected taste cells (grey) and
756 their lysosomes (color coded by size from small (blue) to large (red)). Reconstructions
757 are divided into cell types: IV, III, II, I, early dying (**ed**), and late dying (**ld**). **B.** Lysosome
758 count per cell (left) and lysosome median volume by cell (right). Each data point
759 represents a single cell. Data is binned by cell type, as in **A. C.** Swarm charts of lysosome
760 volumes of healthy Type II cells and early stage dying Type II cells showing the entire
761 range of volumes (left) and a cropped view (right) of the volumes below 1µm^3. Black
762 squares indicate mean volume, while diamonds indicate median volume. **D.**
763 Reconstructions of the lysosome meshes from healthy Type II cells (blue) and an early

764 stage dying Type II cells (purple). Inset shows an enlarged view of the perinuclear area
765 from a healthy and dying cell.
766 **Figure 5. Morphological features of healthy and dying taste cell nuclei. A.**
767 Reconstruction of healthy Type II cell nucleus (blue) with distended regions between
768 inner and outer nuclear membranes reconstructed in gray. **B.** Micrograph of a healthy
769 Type II cell nucleus (that reconstructed in **A**) (blue, left) and a nucleus of a dying Type II
770 cell on the right (purple) showing distended regions between the inner and outer
771 nuclear membrane. Scale bar is 2 µm, and applies to all micrographs in this figure. **C.**
772 Reconstruction of the nucleus shown in **B**, showing in the inner nuclear region in purple,
773 and the distended regions between the inner nuclear membrane in lighter purple. Of
774 the dying cell nuclei, this is the only nucleus for which these distended regions were
775 segmented and reconstructed. Thus, the reconstructions in **E** and **G** do not feature
776 equivalent reconstructions of the distended nuclear membrane regions**. D, D'.**
777 Reconstruction (**D**) and micrograph (**D'**) of healthy Type II cell nucleus. **E, E'.**
778 Reconstruction (**E**) and micrograph (**E'**) of a fragmented nucleus of a dying cell of
779 unknown type. Arrows indicate regions of heterochromatin expansion. **F, F'.**
780 Reconstruction (**F**) and micrograph (**F'**) of a healthy Type III cell nucleus. **G, G'.**
781 Reconstruction (**G**) and micrograph (**G'**) of the shrunken nucleus of a dying cell of
782 unknown type. Arrows indicate regions of heterochromatin expansion.
783
784 **Figure 6. Synapses in dying cells. A.** Micrograph of the point of contact between a late
785 stage dying cell of unknown type (purple) and an adjacent nerve fiber (yellow). Asterisk

786 indicates region of contact. Scale bar is 1 µm and applies to all micrographs in this
787 figure. **B.** Synaptic sites between two nerve fibers (yellow-green and yellow) and a dying
788 Type II cell (purple). Arrows indicate atypical mitochondria (red), which feature
789 abnormal cristae patterns. **C.** Reconstruction of a dying Type II cell (purple) and the
790 three nerve fibers that receive synapses from it in the taste bud shell (gray). Atypical
791 mitochondria are red. Only the orange fiber exits the base of the taste bud. The green
792 and pink fibers appear to be nerve fiber fragments. Scale bar 10 µm. **D.** Micrograph
793 showing a region of contact between a dying Type III cell (purple) and the adjacent
794 nerve fiber (yellow). **E.** Enlarged micrograph showing a different point of contact
795 between the dying Type III cell (purple) and the nerve fiber (yellow) in **D**. Arrows
796 indicate large, swollen structures (upper arrow) and typical synaptic vesicle structures
797 (lower arrow) at the point of contact with the nerve fiber. **F.** Reconstruction of a dying
798 Type III cell (purple) and the nerve fiber it borders. This nerve fiber is a fragment and
799 does not exit the base of the bud.
800
801 **Figure 7. Type I cells as they relate to dying cells. A.** Reconstruction of a late stage dying
802 cell (purple) and the two Type I cells (green) that surround it. **B.** Micrograph of an early
803 stage dying Type II cell (purple) and a neighboring Type I cell (green). Asterisk indicates a
804 region of the dying cell nearly surrounded by the neighboring Type I cell, likely an area
805 of phagocytosis. **C.** Micrograph of a late stage dying cell (purple) and the bordering Type
806 I cell (green). Arrow indicates a presumed apoptotic body, which is completely
807 surrounded by the Type I cell. **D.** Reconstruction of a late stage dying cell (purple) and

808 the neighboring Type I cell (green). Lysosomes in the Type I cell are depicted in pink. **D'.**
809 Rotated, enlarged view of the Type I cell partially surrounding the dying cell. **D''.**
810 Enlarged region of D which highlights the lysosomes (pink) in the region of the Type I cell
811 that borders the dying cell. **D'''.** Enlarged region of D which highlights the lysosomes
812 (pink) in the region of the Type I cell that does not border the dying cell. **E.** Micrograph
813 of a Type I cell (green) that borders an early dying cell (purple). Arrows indicate large,
814 membrane enclosed profiles that the Type I cell may have engulfed from the dying cell.
815 **E'.** Enlarged region of E which highlights the membrane continuity between the dying
816 cell and one such profile that is perhaps in the process of being engulfed by the
817 neighboring Type I cell.
818
819 **Figure 8. Dying cells in the context of the bud. A.** Pie charts depicting the cell type
820 composition of two taste buds: TF21 TB1 and TF21 TB2. These two taste buds are the
821 only taste buds that are fully contained in the boundaries of the tissue block. **B.** Diagram
822 depicting the locations of cell nuclei within the taste bud TF21 TB2 according to cell
823 type. Immature Type IV cell nuclei (pink-purple) are on the left, followed by Type III cell
824 nuclei (red), Type II cell nuclei (blue), Type I cell nuclei (green) and dying cell nuclei
825 (dusty purple). One nucleus in the Type II cell panel is labeled as purple (asterisk),
826 because the cell it inhabits is immature and we cannot discern whether it would have
827 developed into a Type II or Type III cell. The taste bud and nuclei are shown in profile
828 (top row) and from a top down view of the taste bud (bottom).
829

830 **Figure 9. Pathway to death.** Reconstructions of cells summarizing the pathway from
831 birth to death of a taste cell. From left to right: dividing basal cell, Type IV immature
832 taste cell, Immature Type II or III taste cell, Type II mature taste cell, Type II early stage
833 dying cell, Late stage dying cell of unknown type.
834
835 **Supplementary Figure 1. Estimation statistics for the median difference of cell**
836 **volumes between cell categories.** The median differences between healthy and late
837 stage dying cells (**A**); early stage and late stage dying cells (**B**); healthy Type II and early
838 stage dying Type II cells (**C**); and healthy Type III and early stage dying Type III cells (**D**) as
839 shown in Gardner-Altman estimation plots generated using estimationstats.com (Ho et
840 al., 2019). For each comparison, both groups are plotted on the left axes; the mean
841 difference is plotted on a floating axes on the right as a bootstrap sampling distribution.
842 The mean difference is depicted as a dot; the ends of the vertical error bar (black)
843 indicate the 95% confidence interval. All calculated confidence intervals indicate that
844 the compared groups are different.

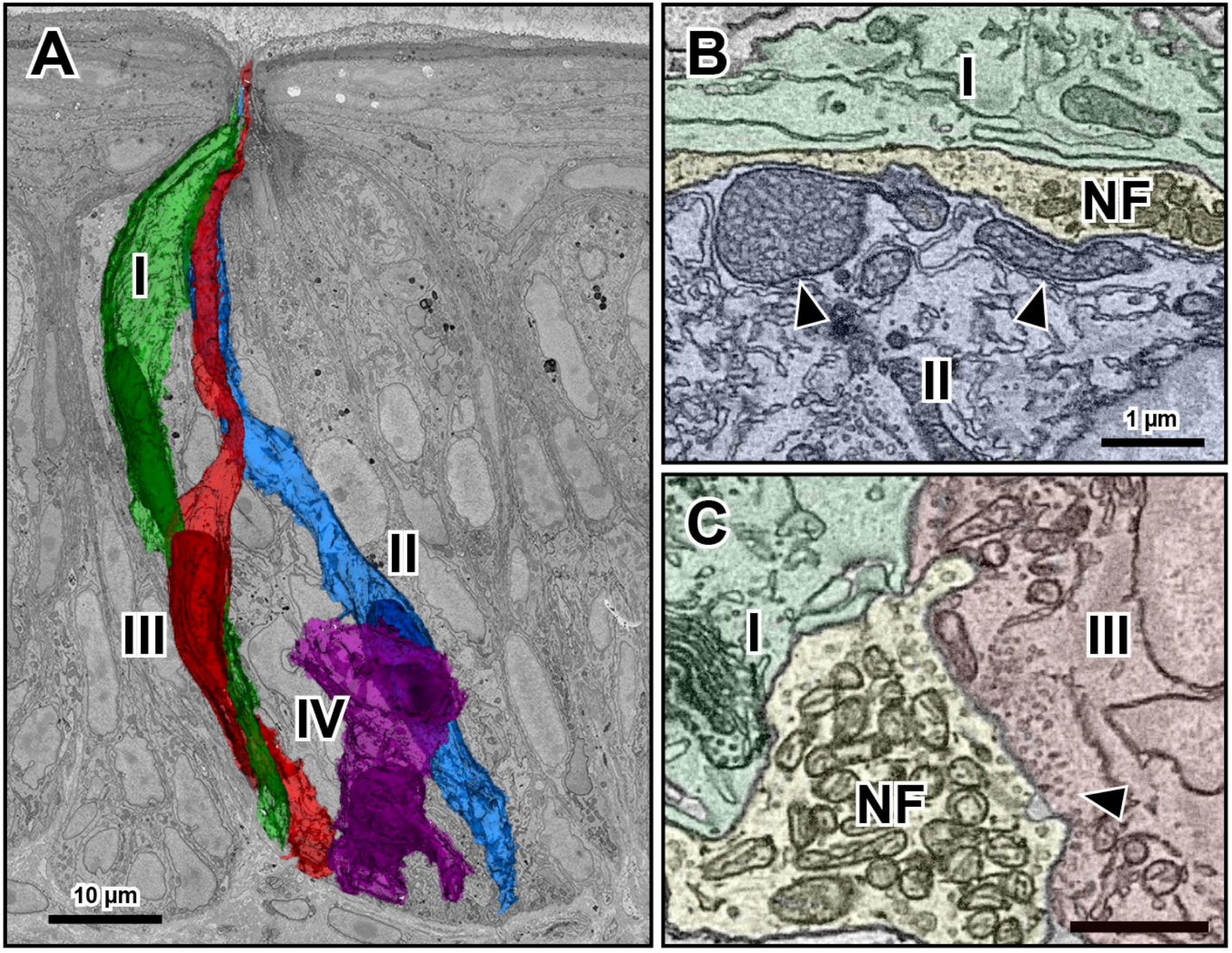
A
I
II
III
IV
10 µm
B
I
NF
II
1 µm
C
I
III
NF

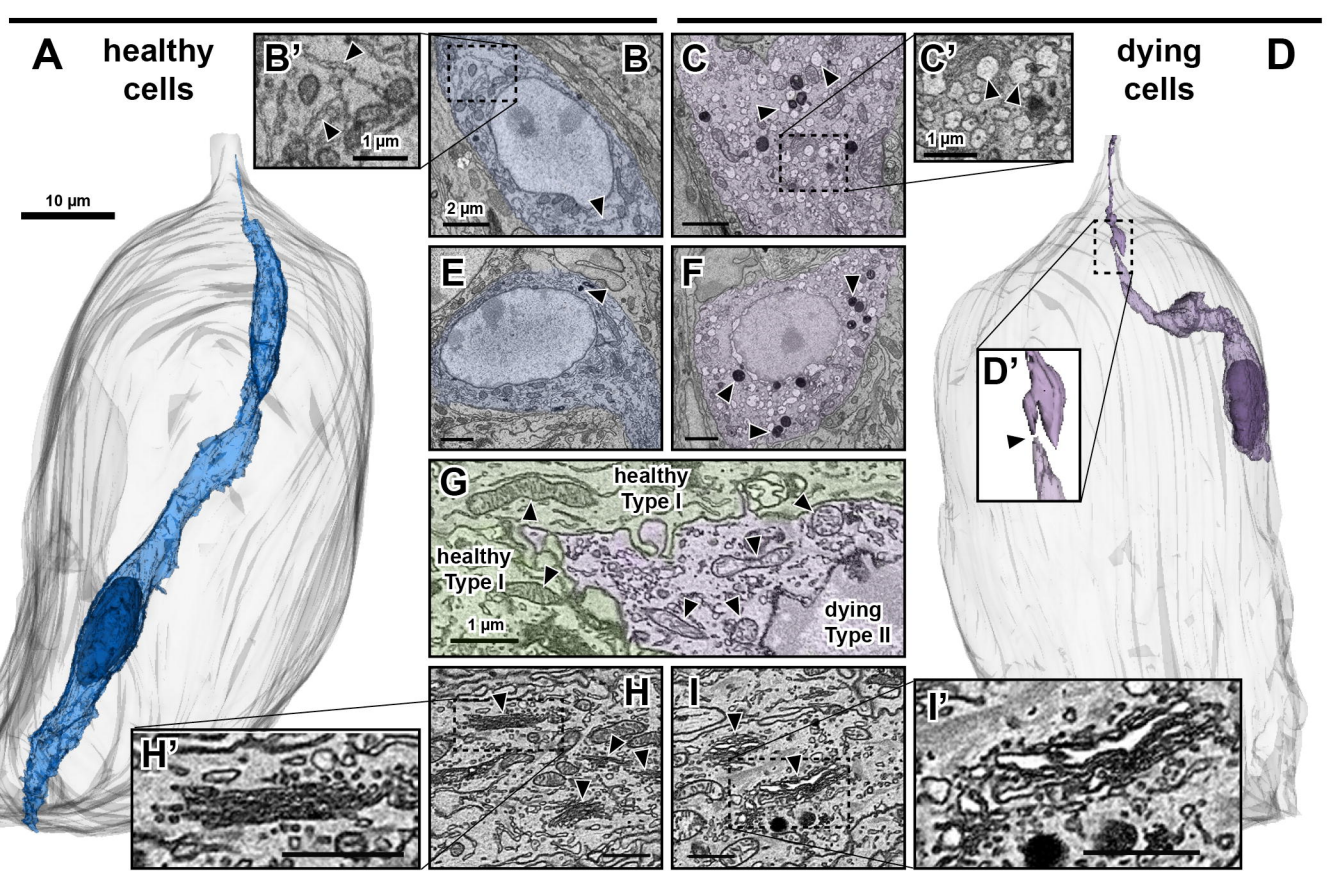
A
healthy cells
B'
1 µm
B
2 µm
C
C'
1 µm
dying cells
D
10 µm
E
F
G
healthy Type I
healthy Type I
1 µm
dying Type II
D'
H'
H
I
I'

Cell Volumes

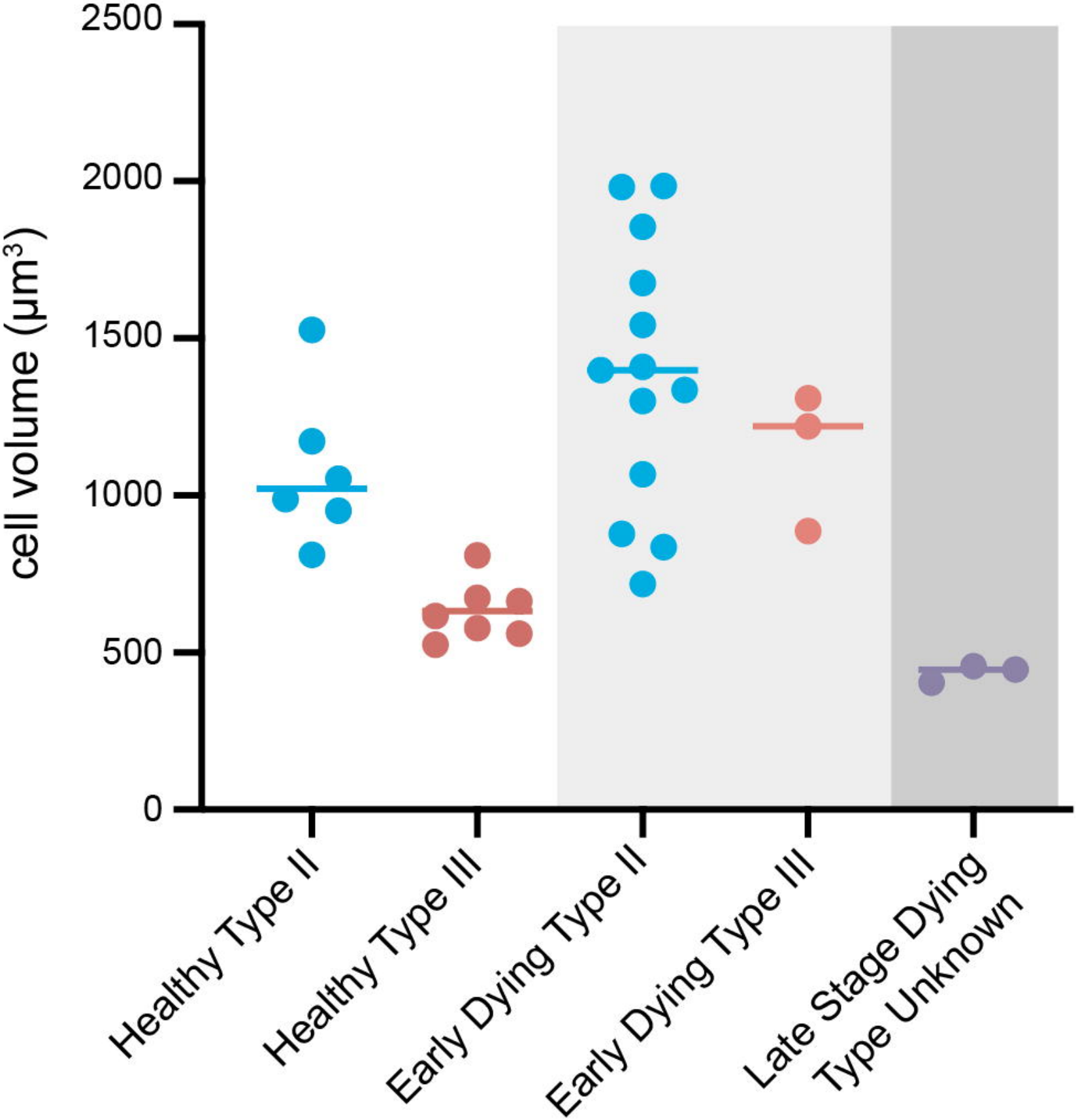

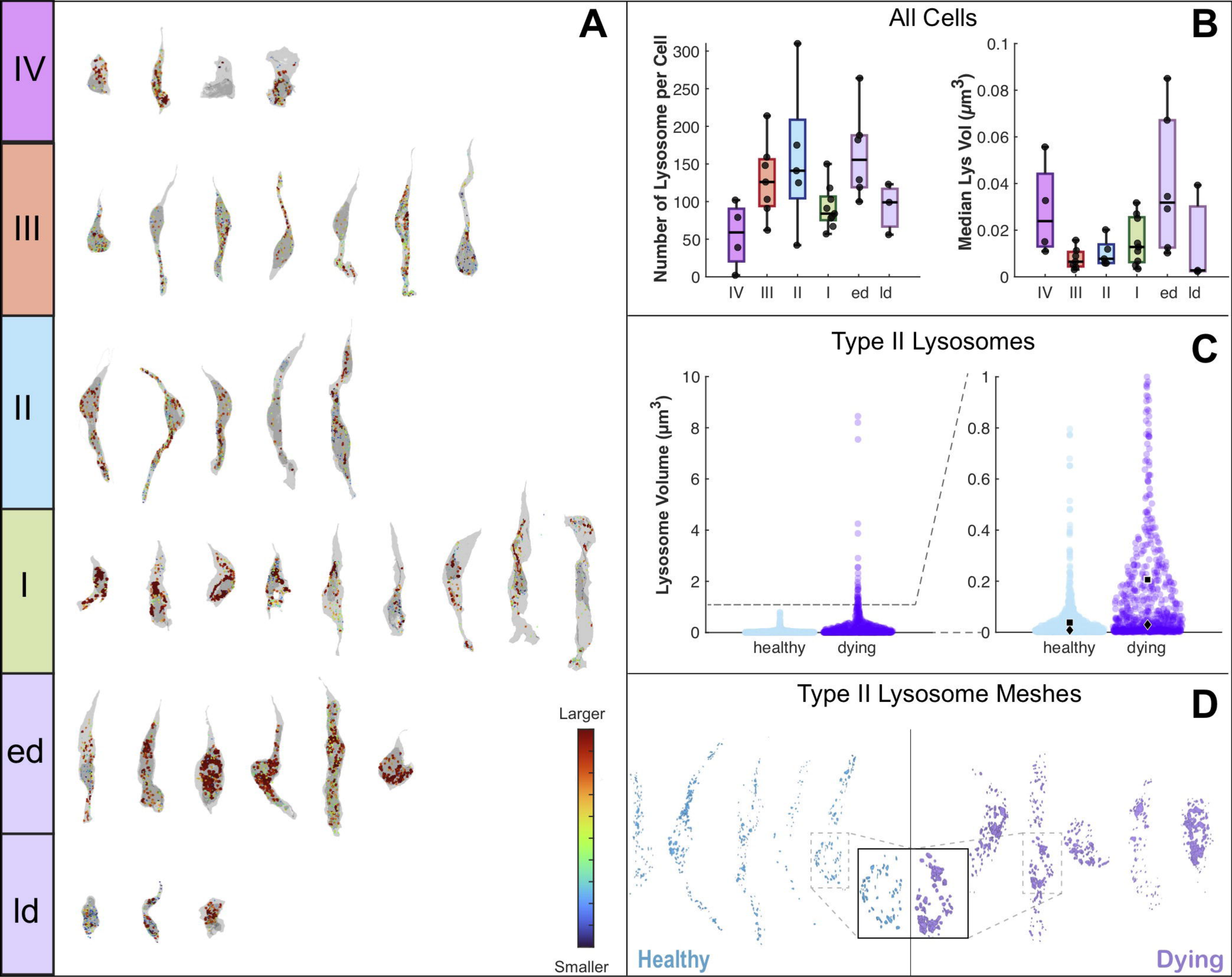
A
IV
III
II
I
ed
ld
Larger
Smaller
All Cells
B
Number of Lysosome per Cell
300
250
200
150
100
50
0
IV III II I ed ld
Median Lys Vol (μm3)
0.1
0.08
0.06
0.04
0.02
0
IV III II I ed ld
Type II Lysosomes
C
Lysosome Volume (μm3)
10
8
6
4
2
0
healthy dying
1
0.8
0.6
0.4
0.2
0
healthy dying
Type II Lysosome Meshes
D
Healthy
Dying

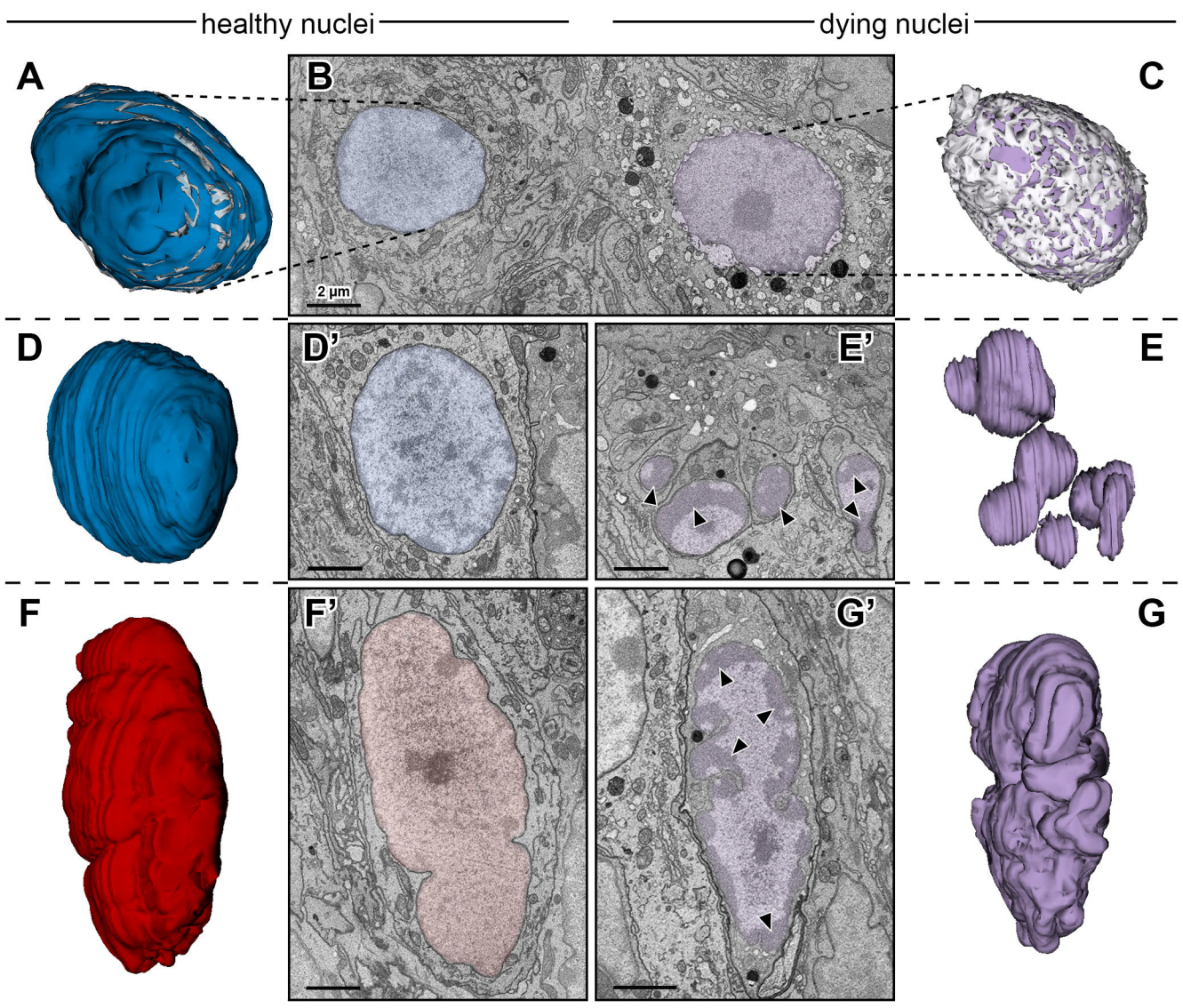
healthy nuclei
dying nuclei
A
B
C
2 µm
D
D'
E'
E
F
F'
G'
G

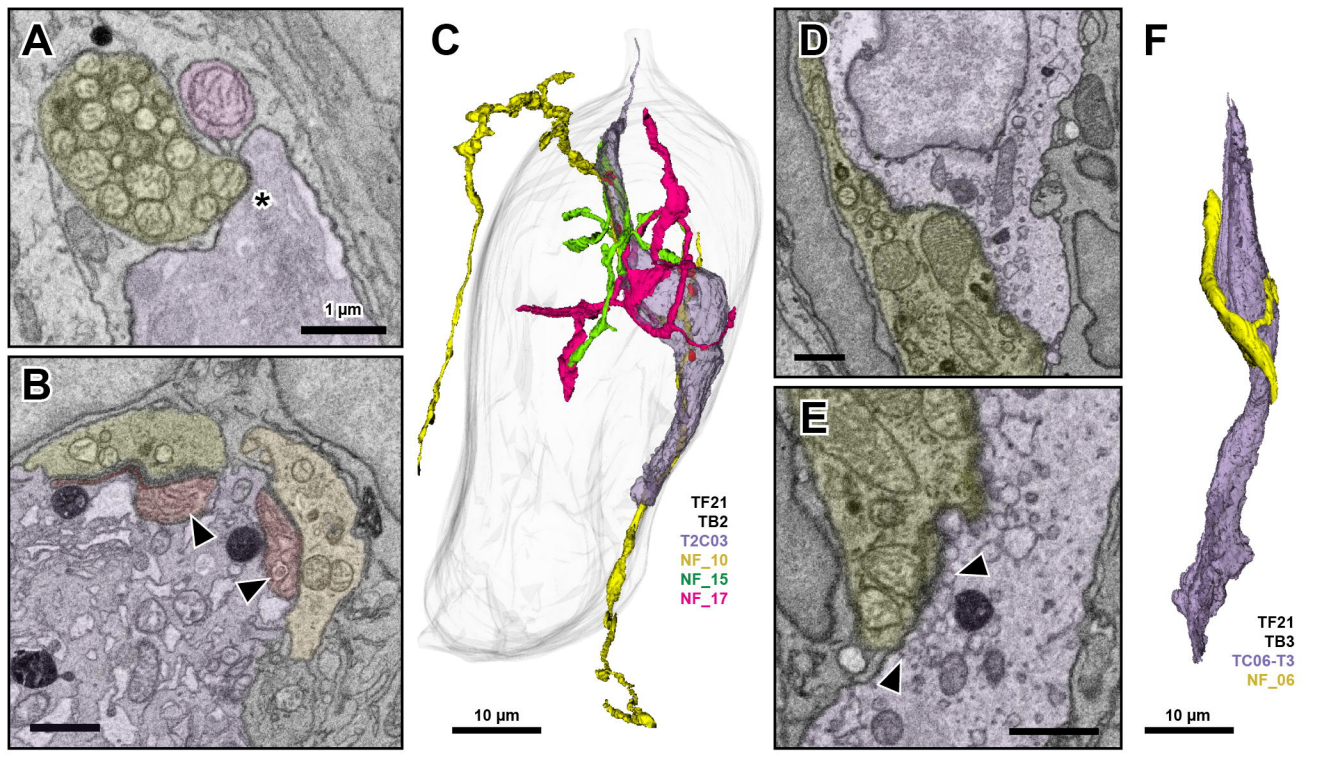
A
*
1 µm
B
C
TF21
TB2
T2C03
NF_10
NF_15
NF_17
10 µm
D
E
F
TF21
TB3
TC06-T3
NF_06
10 µm

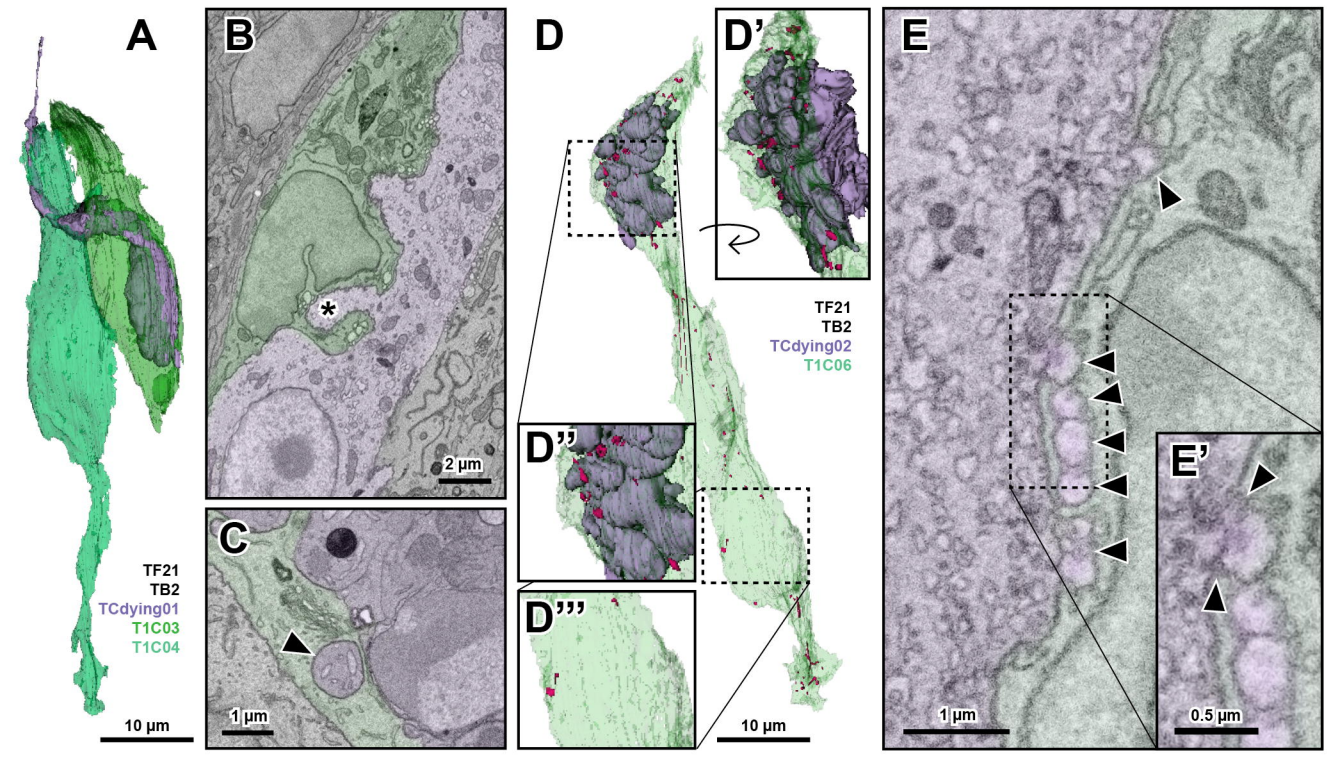
A
TF21
TB2
TCdying01
T1C03
T1C04
10 µm
B
*
2 µm
C
1 µm
D
TF21
TB2
TCdying02
T1C06
10 µm
D'
D''
D'''
E
1 µm
E'
0.5 µm

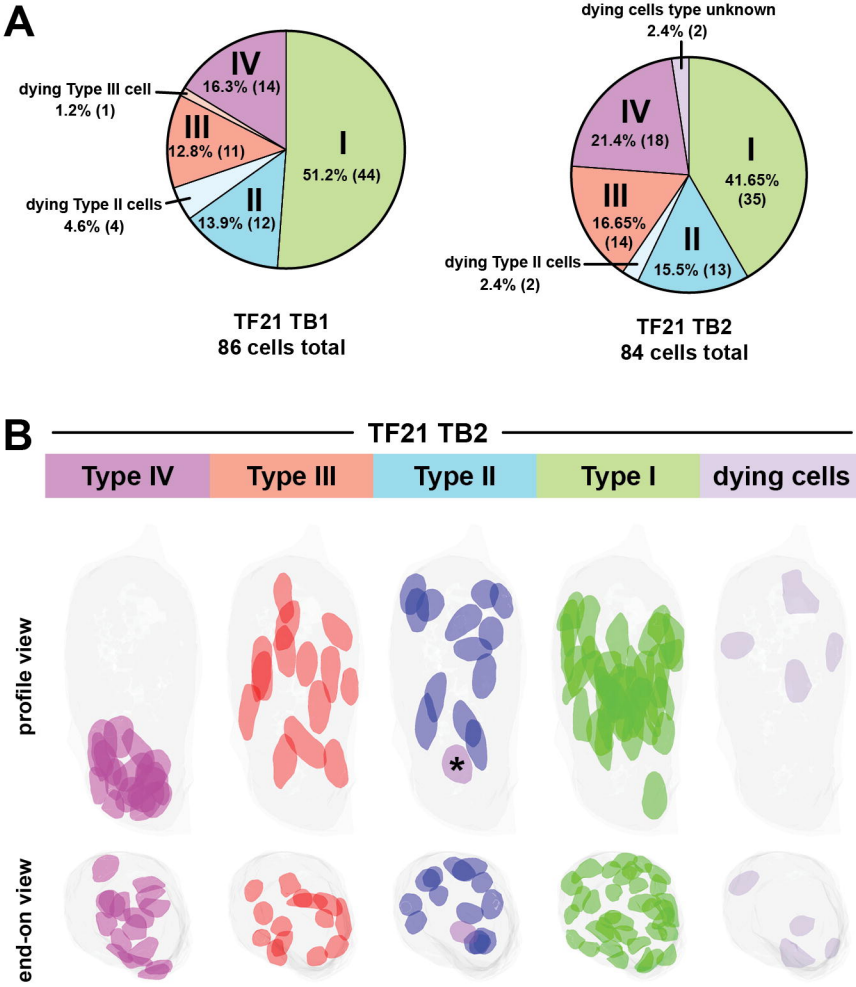
A
IV
16.3% (14)
dying Type III cell
1.2% (1)
III
12.8% (11)
dying Type II cells
4.6% (4)
II
13.9% (12)
I
51.2% (44)
TF21 TB1
86 cells total
dying cells type unknown
2.4% (2)
IV
21.4% (18)
I
41.65%
(35)
III
16.65%
(14)
II
15.5% (13)
dying Type II cells
2.4% (2)
TF21 TB2
84 cells total
B
TF21 TB2
Type IV
Type III
Type II
Type I
dying cells
profile view
end-on view
*

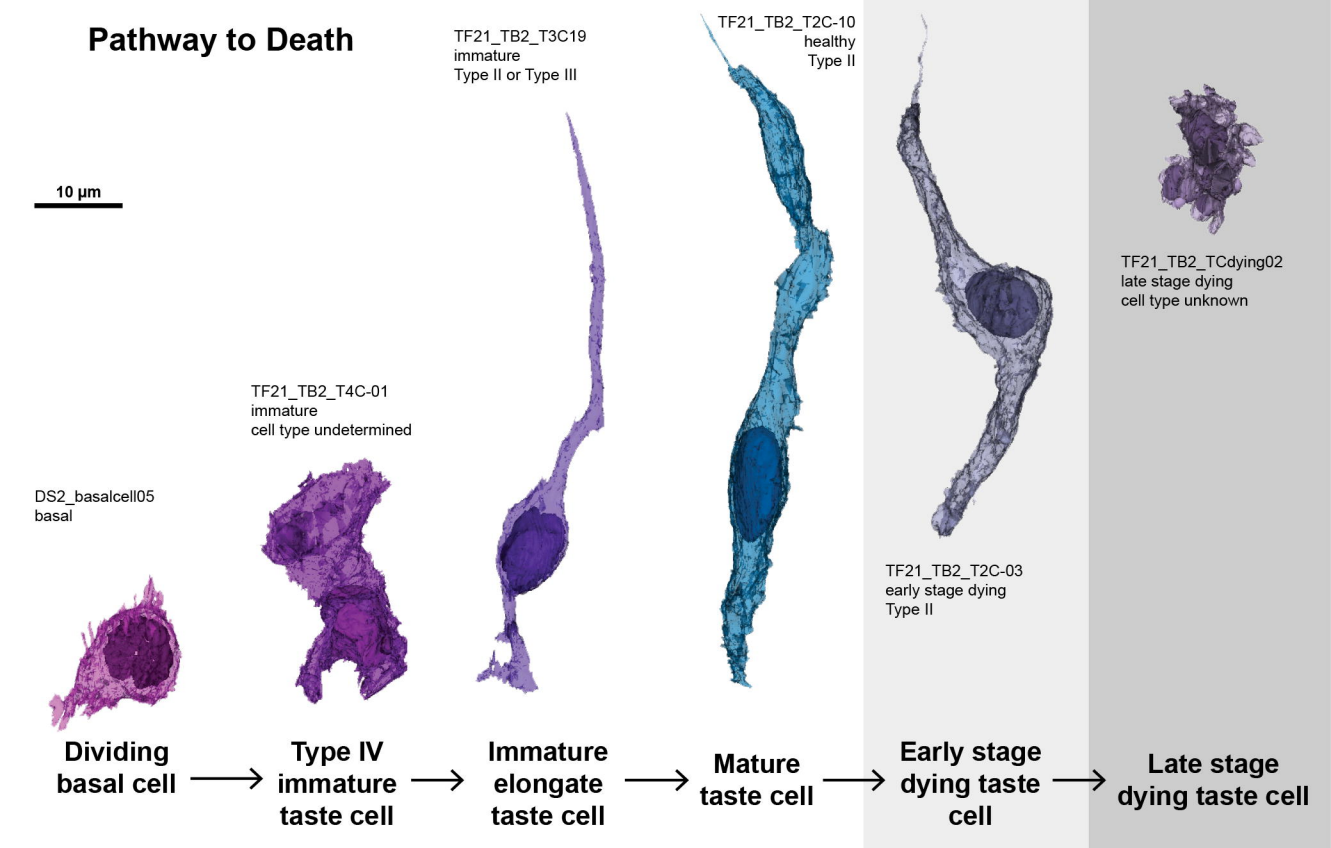
Pathway to Death
10 µm
DS2_basalcell05
basal
TF21_TB2_T4C-01
immature
cell type undetermined
TF21_TB2_T3C19
immature
Type II or Type III
TF21_TB2_T2C-10
healthy
Type II
TF21_TB2_T2C-03
early stage dying
Type II
TF21_TB2_TCdying02
late stage dying
cell type unknown
Dividing basal cell
Type IV immature taste cell
Immature elongate taste cell
Mature taste cell
Early stage dying taste cell
Late stage dying taste cell